

Inverse Determination of Steady Heat Convection Coefficient Distributions

T. J. Martin

Graduate Research Assistant.
Student Mem. ASME

G. S. Dulikravich

Associate Professor.
Fellow ASME
FT7@PSU.EDU

Department of Aerospace Engineering,
The Pennsylvania State University,
University Park, PA 16802

An inverse Boundary Element Method (BEM) procedure has been used to determine unknown heat transfer coefficients on surfaces of arbitrarily shaped solids. The procedure is noniterative and cost effective, involving only a simple modification to any existing steady-state heat conduction BEM algorithm. Its main advantage is that this method does not require any knowledge of, or solution to, the fluid flow field. Thermal boundary conditions can be prescribed on only part of the boundary of the solid object, while the heat transfer coefficients on boundaries exposed to a moving fluid can be partially or entirely unknown. Over-specified boundary conditions or internal temperature measurements on other, more accessible boundaries are required in order to compensate for the unknown conditions. An ill-conditioned matrix results from the inverse BEM formulation, which must be properly inverted to obtain the solution to the ill-posed problem. Accuracy of numerical results has been demonstrated for several steady two-dimensional heat conduction problems including sensitivity of the algorithm to errors in the measurement data of surface temperatures and heat fluxes.

Introduction

A well-posed thermal boundary value problem requires either temperature or heat flux specified over the entire boundary of the solid region. When the surface is exposed to a moving fluid, convective heat transfer coefficients can be utilized as boundary conditions. Accurate values of the convective heat transfer coefficients are difficult to obtain experimentally because their values depend strongly on at least twelve variables or eight nondimensional groups (White, 1988). Typical semi-empirical expressions for prediction of heat convection coefficients represent curve fits through experimental data for very simple configurations covering only limited ranges of flow-field parameters. Consequently, in most practical situations, the heat convection problems are solved by using a single value of the heat convection coefficient on the entire surface exposed to a moving fluid.

This paper offers an entirely different approach to a problem of predicting the surface variation of the heat convection coefficient. The most innovative aspects of this approach are that it does not require any information about the flow-field and that it is noniterative. In other words, it is possible to treat the heat convection coefficient determination problem as an ill-posed boundary value heat conduction problem where no thermal data are available on parts of the boundary exposed to a moving fluid. This approach is capable of utilizing over-determined thermal measurements involving temperatures and heat fluxes where they are accessible. These data are then used to predict distributions of temperature, heat fluxes, and convective heat transfer coefficients on the boundaries where they are unknown.

A noniterative algorithm has been developed that reliably and efficiently solves inverse (ill-posed) boundary condition problems governed by the Laplace equation in two-dimensional and three-dimensional multiply connected domains having different thermal material properties (Martin and Dulikravich, 1996; Dulikravich and Martin, 1996). An extended version of this method was also successfully used in solving ill-posed

problems in two-dimensional elasticity (Martin et al., 1994) as well as for the determination of heat sources (Martin and Dulikravich, 1996). This technique is based on the Green's function solution method, commonly referred to as the Boundary Element Method (BEM). It is an integral technique that generates a set of linear algebraic equations with unknowns confined only to the boundaries. For well-posed problems, Gaussian elimination or any other standard matrix inverter can solve the resulting solution matrix. When an ill-posed problem is encountered, the matrix becomes ill-conditioned. It has been shown that the proper solution to this matrix provides accurate results to various steady inverse heat conduction boundary value problems (Martin and Dulikravich, 1996, 1997). This method has been shown to suppress the amplification in measurement errors in the input data while both minimizing the variance in the output and preventing output bias. The algorithm is applicable to complex, multiply connected two and three-dimensional configurations.

Numerical Formulation

The governing partial differential equation for steady-state heat conduction in a two-dimensional solid with a constant coefficient of thermal conductivity is

$$k\nabla^2 T = 0. \quad (1)$$

This linear elliptic partial differential equation can be integrated subject to Dirichlet (temperature) boundary conditions, Neumann (heat flux) boundary conditions, and, when a boundary is exposed to a moving fluid, the Robin (convective heat transfer) boundary conditions given as

$$-k \frac{\partial T}{\partial n} \Big|_{\Gamma_{\text{conv}}} = h_{\text{conv}}(T|_{\Gamma_{\text{conv}}} - T_{\text{amb}}). \quad (2)$$

When ill-posed boundary value problems are encountered, portions of the boundary must be over-specified with both temperatures and heat fluxes, while nothing is known on boundary Γ_{conv} . Such linear boundary value problems can be solved noniteratively when using the BEM. Consequently, the BEM is more robust than the widely used iterative numerical solution tech-

Contributed by the Heat Transfer Division and presented at the National Heat Transfer Conference, Baltimore, Maryland, August 8-12, 1997. Manuscript received by the Heat Transfer Division April 7, 1997; revision received January 5, 1998. Keywords: Conduction, Conjugate Heat Transfer, Mixed Convection. Associate Technical Editor: R. D. Boyd.

niques. Analytical solutions to the partial differential equation, in the form of the Green's function, are part of the BEM solution. Therefore, high accuracy is expected because introducing the Green's functions does not introduce any error into the solution. In addition, the noniterative nature of the BEM eliminates stability, numerical dissipation, and iterative convergence problems. This is valuable because iterative procedures for the solution of inverse problems tend to amplify errors due to ill-posedness of the iteration matrix thus requiring complex regularization (smoothing) algorithms (Tikhonov and Arsenin, 1977).

The BEM is a standard numerical technique that can be found in a number of textbooks (Brebbia and Dominguez, 1989). Consequently, only pertinent concepts will be summarized in this paper. Since the objective is strictly solving a boundary value problem, the unknown temperature, T , and the unknown flux, Q , are on the boundary Γ_{conv} that is a part of the overall boundary Γ . The boundary Γ can be discretized into N_{BE} isoparametric boundary elements. Although these test cases will not be discussed in this paper (Martin and Dulikravich, 1996), internal measurement points could exist where temperature data are obtained. The T and Q can vary between the neighboring end-nodes defining each boundary element. Each boundary element can be integrated numerically using a standard Gaussian quadrature integration formula. Boundary elements containing a singularity at one end-point can be integrated analytically, resulting in a set of boundary integral equations, one for each boundary node plus one for every possible internal temperature measurement. The resulting discretized form of the BEM can be represented in matrix form (Brebbia and Dominguez, 1989) as

$$[\mathbf{H}]\{\mathbf{T}\} = [\mathbf{G}]\{\mathbf{Q}\}. \quad (3)$$

Here, $[\mathbf{H}]$ and $[\mathbf{G}]$ are full matrices containing geometrically defined coefficients.

For a well-posed boundary value problem, every point on the boundary Γ is given one Dirichlet, Neumann, or Robin boundary condition and there are no internal temperature measurements. These boundary conditions are then multiplied by their respective coefficient matrix and collected on the right-hand side to form a vector of known quantities, $\{\mathbf{F}\}$. The left-hand side remains in the standard form $[\mathbf{A}]\{\mathbf{X}\}$. This well-posed system of linear algebraic equations can be solved for the vector of unknown quantities $\{\mathbf{X}\}$ on the boundary by any standard matrix solver such as Gaussian elimination or LU factorization.

If the boundary conditions (T , Q , or h_{conv}) are unknown on parts of the boundary or if internal temperature measurements are included in the analysis, the problem becomes ill-posed. A solution of this inverse problem of determination of unknown boundary conditions may be obtained by using a procedure explained by Dulikravich and Martin (1996) and Martin and Dulikravich (1996).

In summary, after multiplying the known quantities in the vectors $\{\mathbf{T}\}$ and $\{\mathbf{Q}\}$ by their respective coefficient matrix

columns, the products should be collected into the vector of known quantities, $\{\mathbf{F}\}$. The unknown boundary values of the vectors $\{\mathbf{T}\}$ and $\{\mathbf{Q}\}$ then form a single vector, $\{\mathbf{X}\}$, multiplied by a highly ill-conditioned coefficient matrix, $[\mathbf{A}]$, which is, in general, not square. The truncated Singular Value Decomposition (SVD) method (Press et al., 1986) has been often used to solve this ill-conditioned system of algebraic equations. Very small singular values of such ill-conditioned matrix $[\mathbf{A}]$ are zeroed out so that those algebraic terms that are dominated by noise and round-off error are eliminated from the matrix. In order to determine which singular values are to be truncated, it is necessary to provide a user-specified singularity threshold parameter, τ_{SVD} . One method for determining the most suitable value of τ_{SVD} has been suggested by Martin and Dulikravich (1996). Any singular value, whose ratio with the largest singular value is less than this singularity threshold, will be automatically zeroed out in the SVD algorithm.

In addition to the SVD algorithm, Tikhonov's regularization (Tikhonov and Arsenin, 1977) was also applied in a number of test cases in this study. The observation was that Tikhonov's regularization produces unacceptable levels of global bias when large regularization parameters are required for a smooth solution. Tikhonov's regularization was found to be very effective when errors were introduced into the surface heat flux measurements (Martin and Dulikravich, 1996).

Results

The equation for the boundary heat flux from the Robin boundary condition was added directly into the linear BEM system (Martin and Dulikravich, 1996; Dulikravich and Martin, 1996). The unknown temperatures were factored together with the other boundary nodal temperatures appearing on the left-hand side of the BEM matrix equation set. After the ill-conditioned coefficient matrix $[\mathbf{A}]$ has been inverted using the SVD algorithm, the unknown boundary values of T and Q were obtained from $\{\mathbf{X}\} = [\mathbf{A}]^{-1}\{\mathbf{F}\}$. Once these thermal boundary values were determined on the boundary Γ_{conv} , the convective heat transfer coefficients were determined from

$$h_{\text{conv}} = -k \left. \frac{\partial T}{\partial n} \right|_{\Gamma_{\text{conv}}} / (T|_{\Gamma_{\text{conv}}} - T_{\text{amb}}). \quad (4)$$

Here, T_{amb} is considered as known. Two test cases were used to assess the accuracy of the entire noniterative BEM inverse algorithm and its sensitivity to measurement errors in boundary temperatures and heat fluxes.

A square flat plate with side lengths of 1 m was subject to homogeneous Dirichlet boundary conditions ($T = 0^\circ\text{C}$) on three boundaries and a Robin boundary condition ($h_{\text{conv}} = 1.0 \text{ W m}^{-2} \text{ }^\circ\text{C}^{-1}$, $T_{\text{amb}} = 1.0^\circ\text{C}$) on the bottom boundary. The thermal conductivity (k) was $1.0 \text{ W m}^{-1} \text{ }^\circ\text{C}^{-1}$. The analysis or well-posed formulation consisted of the Dirichlet boundary conditions on the top, left, and right boundaries of the plate, and

Nomenclature

$[\mathbf{A}]$ = coefficient matrix multiplying a vector of unknowns

Bi = Biot number = $h_{\text{conv}} L/k$

$\{\mathbf{F}\}$ = vector of known sources and boundary conditions

$[\mathbf{G}]$ = BEM coefficient matrix multiplying nodal fluxes

h_{conv} = convective heat transfer coefficient

$[\mathbf{H}]$ = BEM coefficient matrix multiplying nodal temperatures

k = thermal conductivity

L = characteristic length

N_{BE} = number of boundary elements

Q = normal temperature derivative or flux $\partial T/\partial n$

$\{\mathbf{Q}\}$ = vector of nodal fluxes

R = random number ($0 < R < 1$)

T = temperature

$\{\mathbf{T}\}$ = vector of nodal temperatures

$\{\mathbf{X}\}$ = vector of unknowns

Γ = boundary contour

σ^2 = statistical variance

τ_{SVD} = SVD threshold value

Ω = domain

Subscripts

amb = ambient fluid quantities

INT = internal measurement

conv = convective heat transfer

perturb = perturbed value

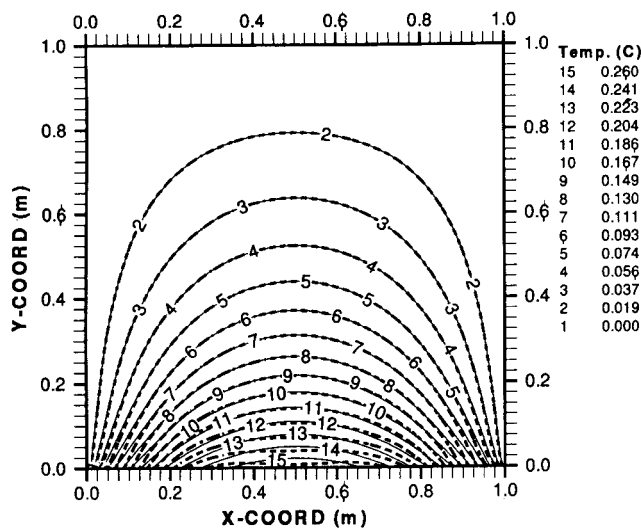


Fig. 1 Isotherms predicted within the rectangular plate by the analytical (solid lines), direct BEM (dotted lines), inverse BEM with top boundary over-specified (dashed lines), and the inverse BEM with top and side boundaries over-specified (dash-dot lines). Forty panels per side.

the Robin boundary condition on the bottom boundary. Using separation of variables, an analytical solution for this test case can be found in the following form (where a and b are the side lengths):

$$T(x, y) = \frac{2h_{conv}}{a} \sum_{n=1}^{\infty} \left[\int_0^a T_{amb} \sin\left(\frac{n\pi x}{a}\right) dx \right] \times \frac{\sinh\left(\frac{n\pi(b-y)}{a}\right) \sin\left(\frac{n\pi x}{a}\right)}{h_{conv} \sinh\left(\frac{n\pi b}{a}\right) + \frac{n\pi k}{a} \cosh\left(\frac{n\pi b}{a}\right)} \quad (5)$$

The BEM analysis predicted the heat fluxes on the top, left, and right boundaries, and temperature on the bottom boundary. When the entire computed temperature field was plotted (Fig. 1), the isotherms (thin dashed lines) obtained numerically using the BEM analysis were practically identical to the analytically obtained isotherms (full lines), having an error of less than 0.1 percent. This confirmed the very high accuracy of the analysis version of the BEM code used in this study.

The inverse problem was then formulated by specifying nothing on the bottom boundary of the rectangular plate while one or more of the remaining boundaries were over-specified with temperatures and heat fluxes taken from the analytical solution. In order to check the performance of the inverse version of the BEM code with respect to the amount of over-specified data, two variations of this numerical test case were performed.

Test Cases With Constant h_{conv} . In the first variation, only the top boundary of the square plate was over-specified with temperature and heat flux, while the side boundaries were specified with temperature only. The isotherms predicted by the inverse noniterative BEM procedure are shown as dotted lines in Fig. 1. The ambient fluid temperature was considered to be known ($T_{amb} = 1.0^\circ\text{C}$). Therefore, the convective heat transfer coefficients can be computed directly after both the temperature and heat flux on the bottom boundary have been predicted.

The computed convective heat transfer coefficients on the bottom boundary, which in this test case should be $h_{conv} = 1.0 \text{ W m}^{-2} \text{ }^\circ\text{C}^{-1}$, are plotted as square symbols in Fig. 2. The average error in h_{conv} is less than 1 percent and a peak error is

6 percent in this test case where over-specified data were provided only on a single boundary farthest from the boundary with unknown thermal boundary conditions.

Influence of the Amount of Over-specified Data. In the second variation of this test case, the opposite (top) boundary as well as both side boundaries were over-specified with both temperature and heat flux from the analytical solution. The isotherms that were predicted by the inverse noniterative BEM code are shown as dash-dot lines in Fig. 1. These isotherms cannot be seen because they lie directly on top of the isotherms predicted by the analysis version of the BEM code and by the analytical solution. The numerically predicted values of local h_{conv} from the inverse BEM procedure for this test case are plotted using triangle symbols in Fig. 2. Notice that the prediction of h_{conv} is more accurate in this test case, having a peak error of 0.4 percent. From these results it can be concluded that the inverse BEM prediction of the unknown h_{conv} is sensitive to the amount of over-specified data and the location of the over-specified boundaries.

Influence of Distance of Over-specified Boundary. To clarify that issue further, the aspect ratio ($AR = b/a$) of the rectangular plate was varied while over-specifying only the top boundary, which is the farthest away from the unspecified bottom boundary. From Fig. 3 it can be seen that for relatively thin domains ($AR < 0.25$) the peak error in the predicted h_{conv} is less than 0.3 percent. The peak error increases to approximately 10 percent, as the rectangular plate becomes a square plate (Fig. 3), while the average error remains below 1 percent.

Applicability to Different Values of Biot Number. The previous numerical results were obtained for unity Biot number ($Bi = h_{conv} L/k$). The second variation inverse problem was then repeated for a variety of Biot numbers by utilizing values of the thermal conductivity in the interval $0.01 < k < 100.0 \text{ W m}^{-1} \text{ }^\circ\text{C}^{-1}$, and thus varying the Biot number over the same range since $L = 1.0 \text{ m}$ and $h_{conv} = 1.0 \text{ W m}^{-2} \text{ }^\circ\text{C}^{-1}$ were kept constant. The threshold parameter in the SVD algorithm was $\tau_{SVD} = 10^{-6}$. From Fig. 4 it can be concluded that the standard deviation and maximum error of the predicted h_{conv} were very low for $0 < Bi < 20$, after which the maximum error increased

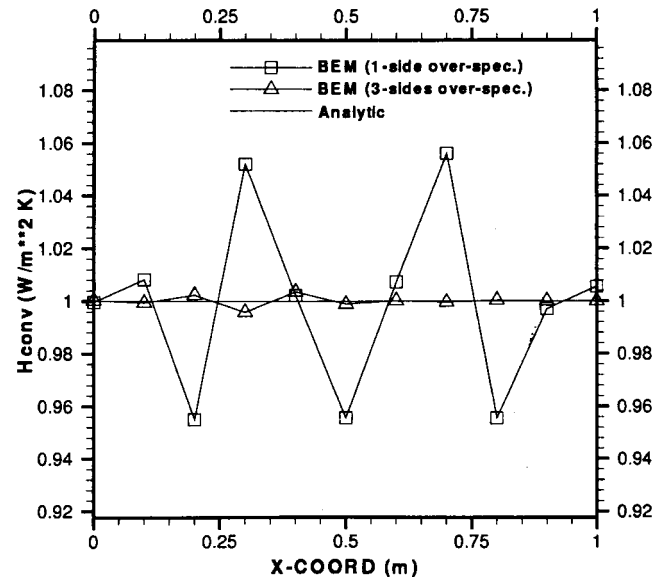


Fig. 2 Convective heat transfer coefficients, h_{conv} , numerically predicted by the inverse BEM on the bottom boundary of a square plate when: (a) the top boundary (squares), and (b) left, top, and right boundaries (triangles) were over-specified. The exact value is $h_{conv} = 1.0 \text{ W m}^{-2} \text{ }^\circ\text{C}^{-1}$. Ten panels per side were used.

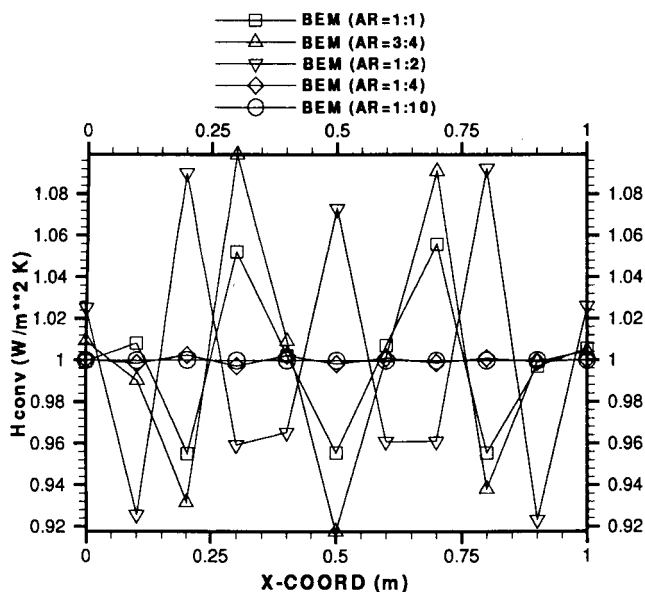


Fig. 3 Influence of the aspect ratio (height/width) of the rectangular plate and the amount of the over-specified data on the numerically predicted h_{conv} on the bottom boundary when: (a) the top boundary (squares), and (b) left, top, and right boundaries (triangles) were over-specified. The exact value is $h_{conv} = 1.0 W m^{-2} \text{ } ^\circ C^{-1}$. Ten panels per side were used.

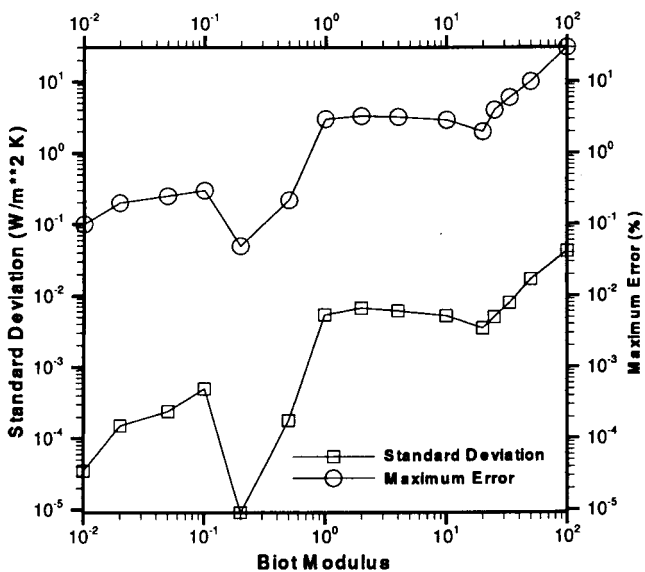


Fig. 4 Influence of Biot numbers on maximum error and standard deviation of the predicted h_{conv}

until it reached 30 percent for $Bi = 100$. For example, a plasma-coated gas turbine blade surface distribution of h_{conv} can be predicted quite accurately with this inverse BEM algorithm. In this example, the coating thickness (L) is $2 \times 10^{-4} m$, and k is $1.0 W m^{-1} \text{ } ^\circ C^{-1}$. If $Bi < 20$, this means that h_{conv} as high as $10^5 W m^{-2} \text{ } ^\circ C^{-1}$ can be predicted with a maximum error of 2 percent and a standard deviation of less than $10^{-2} W m^{-2} \text{ } ^\circ C^{-1}$.

A Test Case With Variable h_{conv} . The inverse BEM algorithm was also evaluated for the more realistic case where the heat convection coefficient is not a constant. The same boundary conditions on the top and the vertical side boundaries were used as in the previous test cases while specifying the variable heat convection coefficient as $h_{conv} = [1.0 + \sin(2\pi x)] W m^{-2} \text{ } ^\circ C^{-1}$ on the bottom boundary. This test case does not have an analyti-

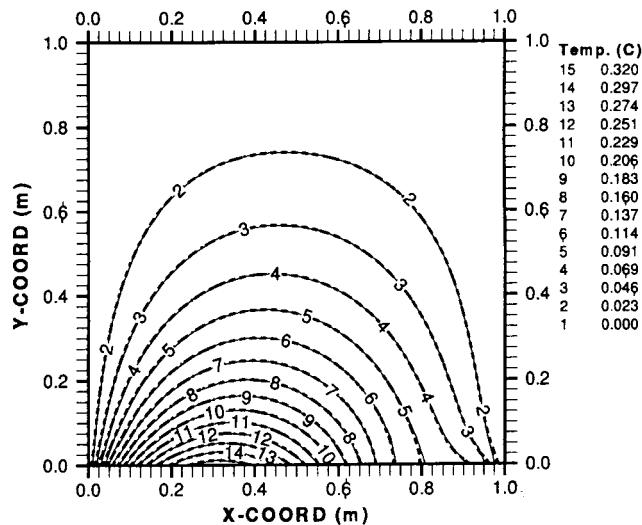


Fig. 5 Isotherms predicted by a well-posed BEM (full lines) and inverse BEM (dashed lines) for the rectangular plate with $h_{conv} = [1.0 + \sin(2\pi x)] W m^{-2} \text{ } ^\circ C^{-1}$ on the bottom boundary and $T = 0.0^\circ C$ on the remaining three boundaries. Forty panels per side were used.

cal solution. Therefore, the BEM analysis code was run with 40 boundary elements on each of the four sides of this well-posed problem and treated the predicted isotherms as the accurate result (Fig. 5).

An inverse problem was then created by pretending that h_{conv} is unknown on the bottom boundary. These "unknown" values of h_{conv} were then predicted by over-specifying the vertical boundaries and the top boundary with the $T = 0.0^\circ C$ and with the heat fluxes that were previously predicted by the BEM solution for the forward problem with sine wave h_{conv} on the bottom boundary. The threshold parameter used in the SVD algorithm had the value $\tau_{SVD} = 10^{-4}$. The result of the inverse BEM code was a highly accurate temperature field shown as dashed lines in Fig. 5 that practically coincide with the solid lines predicted by the well-posed problem solution. An equally accurate prediction of the sine wave h_{conv} variation on the lower boundary (dashed line in Fig. 6) thus confirms the high accuracy and the applicability of this inverse BEM algorithm to prediction of variable h_{conv} values.

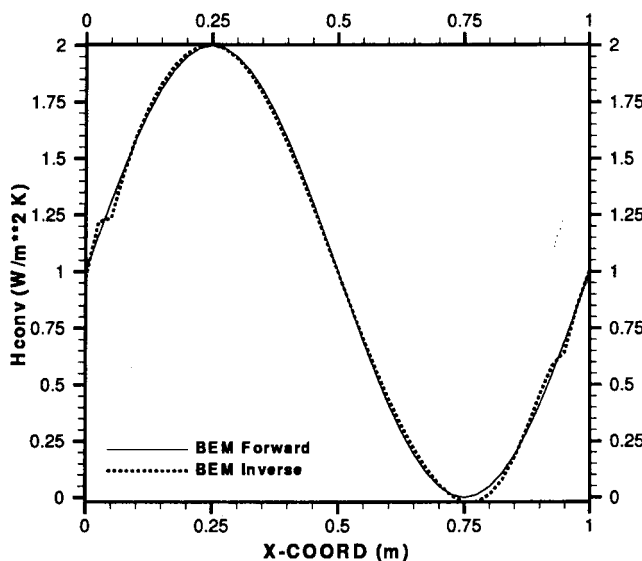


Fig. 6 Analytical (full line) and inverse BEM predicted (dotted line) variation of h_{conv} along the bottom boundary

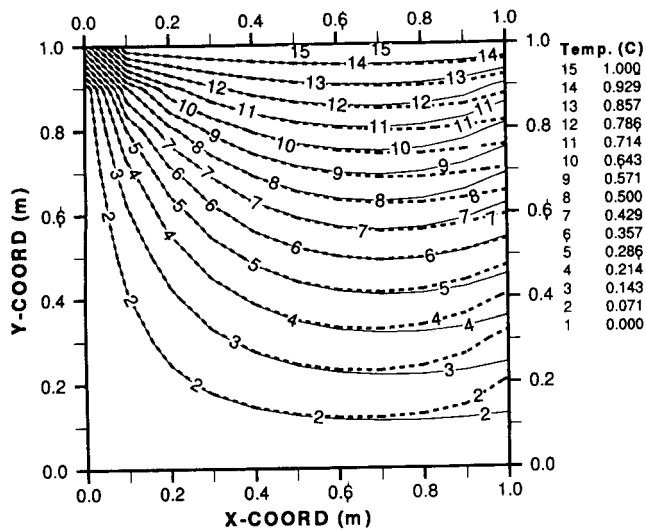


Fig. 7 Isotherms predicted analytically (solid lines) and using analysis BEM (thin dashed lines), inverse BEM with left boundary over-specified (dotted lines), and the inverse BEM with bottom, left, and top boundaries over-specified (dash-dot lines). Ten panels per side were used.

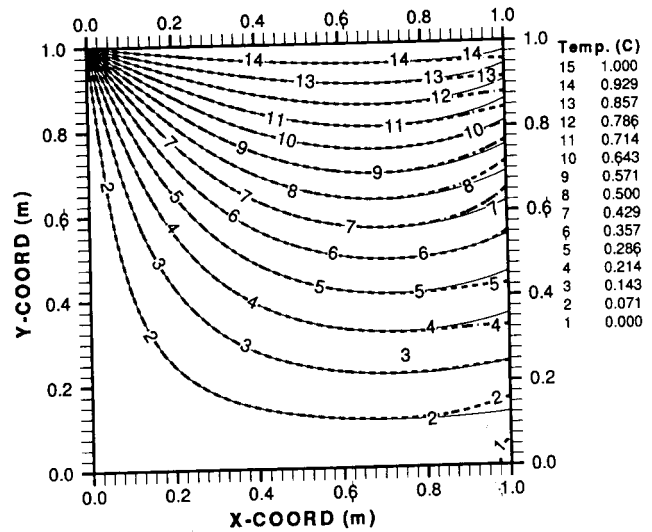


Fig. 8 Isotherms predicted analytically (solid lines) and using analysis BEM (thin dashed lines), inverse BEM with left boundary over-specified (dotted lines), and the inverse BEM with bottom, left, and top boundaries over-specified (dash-dot lines). Forty panels per side were used.

Test Cases With Asymmetric Boundary Conditions. For a second test case, the geometry was a homogeneous square plate with each side of length L discretized with 10 linear isoparametric boundary elements. The boundary conditions were altered such that the right-side boundary had the Robin boundary condition ($h_{conv} = 1.0 \text{ W m}^{-2}\text{C}^{-1}$, $T_{amb} = 0.0^\circ\text{C}$). In the well-posed (analytical) problem, the top boundary was specified with a temperature $T = 1.0^\circ\text{C}$ and the left-side and bottom boundaries were specified with a temperature $T = 0.0^\circ\text{C}$. The analytical solution for this problem can be found by separation of variables, and is given by

$$T(x, y) = \frac{2T_{amb}h_{conv}L}{k} \sum_{n=1}^{\infty} \frac{1 - \cos \alpha_n}{\alpha_n \left(h_{conv} \frac{L}{k} + \cos^2 \alpha_n \right)} \times \frac{\sinh \frac{\alpha_n y}{L}}{\sinh \alpha_n} \sin \frac{\alpha_n x}{L}, \quad (6)$$

where

$$\tan \alpha_n = - \frac{\alpha_n k}{h_{conv} L}. \quad (7)$$

As in the previous test case, the BEM analysis was compared to the analytical solution. The analytically predicted isotherms (solid lines) and the numerical analysis or the well-posed BEM numerical prediction (dashed lines) are directly on top of each other (Fig. 7), thus confirming the high accuracy of the analysis version of the BEM code used in this study.

Again, two variations of the inverse problem were created. One variation had only the left boundary over-specified. The other variation had bottom, left, and top boundaries over-specified. In both inverse variations, nothing was specified on the right-side boundary where heat transfer coefficients were prescribed in the well-posed problem. In the case where only the opposite boundary (left side) was over-specified, the inversely predicted isotherms (dotted lines) show an appreciable error in the vicinity of the unspecified right side boundary (Fig. 7). The error in the inversely predicted isotherms was significantly reduced when a larger quantity of the over-specified data (40

panels per each side of a square) was used (Fig. 8). The value of h_{conv} on the right-side boundary was then obtained from the predicted temperatures and heat fluxes on that boundary (Fig. 9). There was a large discrepancy in the computed h_{conv} values when only the opposite boundary (left-side boundary) was over-specified, since this boundary is far away from the unspecified right-side boundary. The maximum error in predicted h_{conv} was dramatically reduced to about 2 percent when bottom, left-side, and top boundaries were over-specified (Fig. 9).

Sensitivity to Errors in the Input Temperatures. It is of utmost practical importance to assess the influence of measurement errors of boundary values in any newly proposed inverse boundary value determination algorithm. Adding a random error based on the Gaussian probability density distribution to the temperature measurements numerically simulated this effect. A random number, $0 < R < 1$, was generated using a standard

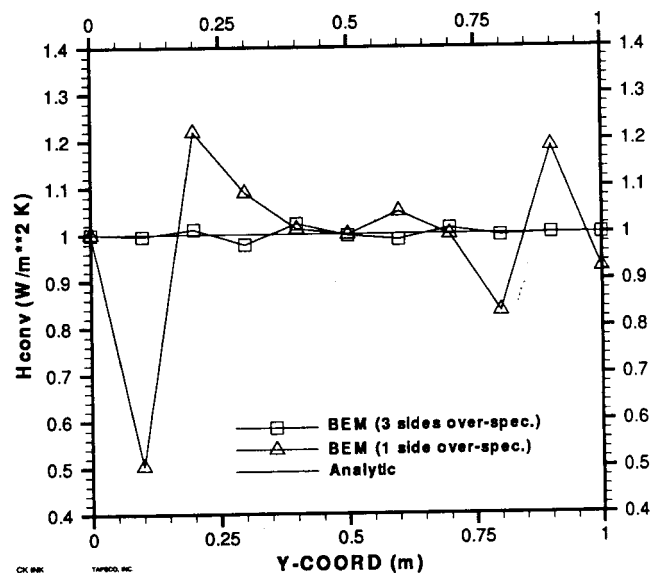


Fig. 9 Convective heat transfer coefficient predicted by the inverse BEM on the right boundary of a square plate when: (a) the left boundary (triangles), and (b) bottom, left, and top boundaries (squares) were over-specified. Ten panels per side were used.

$$T_{\text{perturb}} = T \pm \sqrt{-2\sigma^2 \ln R} \quad (8)$$

Here, addition and subtraction of the random error had a 50–50 chance of been chosen. The errors were assumed to be additive and the same variance was prescribed for all temperature measurements.

This simple test of sensitivity was applied to the second variant of the first test case discussed in this paper with the unknown heat convection on the bottom boundary, while the remaining three sides of the rectangle ($AR = 1$) were over-specified. The input temperatures had intentionally introduced random errors. The predicted values of h_{conv} had a maximum local error of 4 percent when average perturbation was 0.01 percent of T_{max} (Fig. 10). A maximum local error of 8.5 percent was realized when average perturbation was 0.1 percent of T_{max} . It increased to 16 percent when the average perturbation was 1 percent of T_{max} . The maximum local error in predicted h_{conv} reached 33 percent when the average perturbation of supplied (measured) boundary temperature was 10 percent of the maximum temperature in the field. At the same time, it can be seen (Fig. 10) that the average error in the predicted h_{conv} is approximately the same magnitude as the average level of the perturbations (errors) introduced in the boundary temperatures.

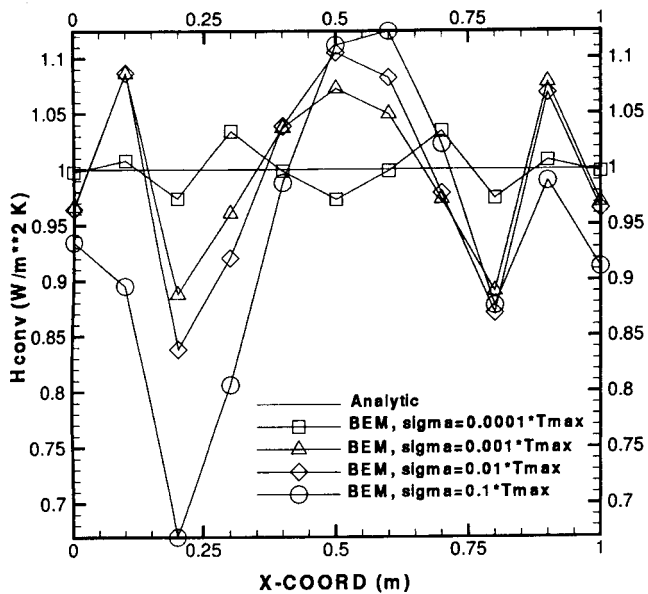


Fig. 10 Sensitivity of the predicted distributions of h_{conv} on the bottom boundary for different standard deviations of the intentionally introduced errors in over-specified temperatures on the remaining three boundaries in the first test case. SVD and ten panels per side were used.

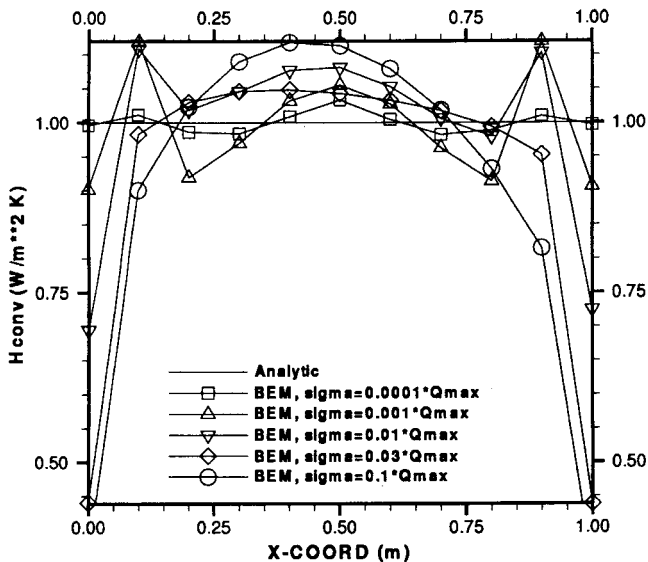


Fig. 11 Sensitivity of the predicted distributions of h_{conv} on the bottom boundary for different standard deviations of the intentionally introduced errors in over-specified fluxes on the remaining three boundaries in the first test case. Tikhonov's regularization and ten panels per side were used.

Sensitivity to Errors in the Input Fluxes. A similar response of this inverse BEM code was obtained when the random errors were intentionally introduced in the input heat fluxes (according to a formula similar to Eq. (8)) on the three over-specified boundaries (Fig. 11). For all practical purposes, there was no net bias in the simulated input measurement errors. For example, when an input error of $0.01 * Q_{\text{max}}$ was introduced, the net bias in the integrated boundary heat flux averaged over each boundary was 5×10^{-6} or 0.05 percent of the unperturbed average heat flux on that boundary. By comparing Figs. 11 and 10, it can be seen that the average error in the predicted values of h_{conv} is somewhat higher in the case with input errors in heat fluxes than in the case with input errors in temperatures. It is remarkable that the level of average error and the peak error in the predicted h_{conv} are of the same order of magnitude as the average errors and the peak errors in the input values of heat fluxes on the over-specified boundary.

In these test cases, Tikhonov's regularization was found to provide better results compared to SVD. Table 1 lists the optimum Tikhonov's regularization parameters, τ_{TIKH} , that were found using numerical experimentation on two different computers for two different levels of BEM discretization and then utilized in the inverse BEM code. Since Tikhonov's regularization acts as an artificial sink of energy, Martin and Dulikravich (1996) demonstrated that higher values of τ_{TIKH} lead to a rapidly increasing bias in the integrated computed heat fluxes. This could be improved significantly by increasing the amount of over-specified data. Figure 12 demonstrates improved results when each boundary was discretized with 40 panels on a higher precision computer (Table 1).

Conclusions

It has been demonstrated how a simple modification to any existing BEM analysis algorithm for the solution of Laplace's equation can transform it into an inverse non-iterative determina-

RANF utility subroutine on Cray C-90 computer. The desired variance σ^2 was specified in the input data and the error was added to the analytical temperature data points, T , according to

Table 1 Various levels of intentional errors in the over-specified boundary heat fluxes and the corresponding Tikhonov's regularization parameters used in the BEM inverse problems: (a) on a PC with 10 boundary elements per side resulting in a condition number of matrix = 7, and (b) on the Cray with 40 boundary elements per side resulting in a condition number of matrix = 14

σ	$0.0001 Q_{\text{max}}$	$0.001 Q_{\text{max}}$	$0.01 Q_{\text{max}}$	$0.03 Q_{\text{max}}$	$0.1 Q_{\text{max}}$
τ_{TIKH} on the Cray	1×10^{-6}	1×10^{-5}	1×10^{-4}	5×10^{-4}	1×10^{-2}
τ_{TIKH} on a PC	5×10^{-7}	5×10^{-4}	5×10^{-3}	5×10^{-2}	2×10^{-1}

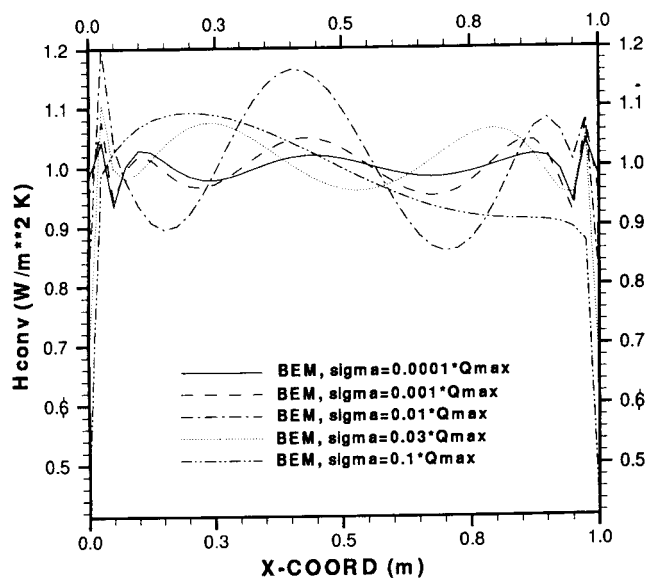


Fig. 12 Sensitivity of the predicted distributions of h_{conv} on the bottom boundary for different standard deviations of the intentionally introduced errors in over-specified fluxes on the remaining three boundaries in the first test case. Tikhonov's regularization and forty panels per side were used.

tion code for unknown distributions of steady convective heat transfer coefficients. This approach is applicable to arbitrarily shaped two and three-dimensional solids where at least part of a boundary can be over-specified with both temperatures and heat fluxes. The code is very fast and robust since it requires inversion of a single fully populated matrix. The inversion must be performed using an algorithm suitable for almost singular matrices. This method is relatively insensitive to the errors introduced in the boundary measurements of temperature while somewhat more sensitive to the errors introduced in the boundary measurements

of heat fluxes. It should be noted that this method for determining unknown steady distribution of heat convection coefficients is inexpensive, since it requires only one temperature probe and one heat flux probe. These two probes can be moved from point to point on accessible boundaries, thus obtaining the over-specified thermal boundary conditions.

Acknowledgments

The authors would like to express their gratitude for the NASA-Penn State Space Propulsion Engineering Center Graduate Student Fellowship, the National Science Foundation Grant DMI-9522854 monitored by Dr. George A. Hazelrigg, the NASA Lewis Research Center Grant NAG3-1995 supervised by Dr. John K. Lytle and Dr. Kestutis Civinskas, and for ALCOA Foundation Faculty Research Fellow Award facilitated by Dr. Yimin Ruan and Dr. Owen Richmond. Special thanks are due to all the reviewers of the original manuscript for their useful suggestions.

References

- Brebbia, C. A., and Dominguez, J., 1989, *Boundary Elements, An Introductory Course*, McGraw-Hill, New York.
- Dulikravich, G. S., and Martin, T. J., 1996, "Inverse Shape and Boundary Condition Problems and Optimization in Heat Conduction," *Advances in Numerical Heat Transfer*, W. J. Minkowycz and E. M. Sparrow, eds., Taylor & Francis, Chap. 10, pp. 324-367.
- Martin, T. J., Halderman, J., and Dulikravich, G. S., 1994, "An Inverse Method for Finding Unknown Surface Traction and Deformations in Elastostatics," *Computers and Structures*, Vol. 56, No. 5, pp. 825-836.
- Martin, T. J., and Dulikravich, G. S., 1996, "Inverse Determination of Boundary Conditions in Steady Heat Conduction With Heat Generation," *ASME JOURNAL OF HEAT TRANSFER*, Vol. 118, pp. 546-554.
- Martin, T. J., and Dulikravich, G. S., 1997, "Non-iterative Determination of Temperature-Dependent Thermal Conductivity," *Symposium on Inverse Design Problems in Heat Transfer and Fluid Flow*, G. S. Dulikravich and K. A. Woodbury, eds., ASME HTD-Vol. 340, Vol. 2, pp. 151-158.
- Press, W. H., Teukolsky, S. A., Vetterling, W. T., and Flannery, B. P., 1986, *Numerical Recipes in FORTRAN, The Art of Scientific Computing*, 2nd ed., Cambridge University Press, Cambridge.
- Tikhonov, A. N., and Arsenin, V. Y., 1977, *Solutions of Ill Posed Problems*, Halsted Press, V. H. Winston & Sons, Washington, DC.
- White, F. M., 1988, *Heat and Mass Transfer*, Addison-Wesley Publishing Company, Reading, MA, p. 272.